AUT Journal of Electrical Engineering
10.22060/EEJ.2026.24404.5701

Innovative Wind Energy System Featuring ANN-Controlled Pitch Regulation for Efficient Grid Integration

Tappeta Amar Kiran[1,*], Dondapati Ravi Kishore[2], Appana Naga Pavani[3], Baswa Uma Maheswari[3], Chappa Sravani Kumari[3]

[1] Associate Professor, Department of Electrical and Electronics Engineering, Godavari Institute of Engineering and Technology (A), Rajahmundry.
[2]Professor, Department of Electrical and Electronics Engineering, Godavari Global University, Rajahmundry.
[3] UG Scholar, Department of Electrical and Electronics Engineering, Godavari Institute of Engineering and Technology (A), Rajahmundry.

[*]Corresponding author Email: amarkiran@giet.ac.in

Abstract:

WECS are dynamic and intricate, considered by uncertainties and external disturbances. This research introduces an innovative pitch control strategy designed to improve energy stabilization and extraction predominantly for WT affected by unmodeled system dynamics to ensure stable operation under high wind speeds. For optimizing power capture, the ANN controller adapts dynamically to changing wind conditions by regulating the turbine blade's pitch angle. For grid integration, a PWM rectifier transforms the variable-frequency AC power from the turbine into DC power. The simulations are conducted in MATLAB/Simulink tool to evaluate the control framework. It reveals that the superior performance of the ANN controller in reducing mechanical loads on turbines and platforms and maximizing power generation. Thus, it achieving reduced power and speed fluctuations, minimal overshoot and enhances the dynamic behaviour of WT.

Keywords:

VSI, WECS, DFIG, Pitch Control by ANN, PWM Rectifier.

10.22060/EEJ.2026.24404.5701

1. Introduction

Due to the rapid urbanization and population expansion, the global demand for energy has surged. The primary energy source is Fossil fuels. Due to the depletion of fossil fuel reserves, many countries face challenges in bridging the gap between energy supply and demand [1].]. Moreover, the wide use of fossil fuels has harmful environmental impacts, comprising contributing to the greenhouse effect. There is a need for new energy sources to meet the ever-increasing need for energy while reducing the adverse effects on the environment [2-5]. Electricity generation from a variety of Renewable Energy Sources (RESs) has garnered a lot of attention in recent years [6]. In particular, wind power is one of the most promising forms in the global energy industry and is anticipated to continue growing quickly over the coming years [7-10]. Control systems need to be incorporated to guarantee the proper wind turbines (WT) operation and efficient utilization of wind energy to optimize power generation output, given the intricacy of wind energy systems and their significant reliance on climatic and environmental conditions. From a control perspective, a key goal is ensuring that the WT's output power remains near its rated level [11]. This is accomplished while minimizing fatigue and vibrations and optimizing efficiency. WT control systems aim to enhance energy production, minimize mechanical loads, stabilize grid integration, and deliver uninterrupted power to the grid. To attain the specified control objectives, optimal control of blade pitch angle and generator torque is essential [12, 13]. The pitch manages the blade’s rotation that regulates the wind's angle of attack to maximize the amount of available wind energy. Pitch control is a leading strategy for boosting power production in medium to large wind turbines among various techniques. The pitch controller focuses on minimizing drag and increasing blade lift within the full-load operational range [14–16]. Fixed pitch stall control and variable pitch control represent two fundamental regulation methods for wind turbines. Variable pitch control maintains rotor speed stability by adjusting the blade pitch angle to match wind speed changes. Unfortunately, the frequent adjustments associated with this method can lead to increased blade stress and pitch servo fatigue, ultimately reducing turbine lifespan [17–18]. The majority of wind turbines currently use Proportional-Integral (PI) controllers because they are straightforward and simple to set up [19]. They

efficiently control the rotor speed, guaranteeing maximum power production even under variable wind conditions. However, PI controllers overestimate blade pitch corrections in windy conditions, which results in instability and higher mechanical stress. By taking into consideration proportional, integral, and derivative actions, the PID controller, which is developed in [20], provides precise control and guarantees steady operation in a range of wind situations. Nevertheless, PID controls struggle to adjust to shifting external circumstances or system dynamics without manual retuning.

The simple optimum intelligent (SOI-PID) controller offers a quick response in numerous functional circumstances. It is better for developing pitch system and assuring the stability of output power in WT. But, it has poor performance and complexity in managing numerous variables and non-linearity [21]. To allow servo motor and vary the pitch angle by the preferred value, the P-PI controller provide the reference pitch signal. However, it is complex to predict the optimal values due to the non-linearity [22]. The pitch controller based on LSTM balance for delay since it derives blade pitch control angle by finding delay occurrence in actuator. It has similar performance during changes in wind speed. Nevertheless, the improper selection lead to oscillation and slow convergence [23]. The conventional controller needs retuning to function over distinct operating points that is less efficient. Also, that controllers are less reliable and has unstable performance in varying conditions. To overcome the above mentioned issues, this research develops an ANN controller based pitch control approach. An ANN controller has the capacity to adapt and learn from data and continuously adjusting its weights to sustain optimal parameters and also provide better robustness to varying conditions. The main objectives are,

- The ANN controller is integrated for regulation of turbine blade pitch angles, enhancing energy efficiency and optimizing electricity generation in response to varying wind speeds.
- For assuring compatibility with grid necessities, the PWM rectifier is exploited to convert variable-frequency AC output from the DFIG to DC power.

- For grid synchronization, improving the compatibility and stability of the power system, a Voltage Source Inverter (VSI) is utilized to convert the DC power back to AC power.

- For enabling steady voltage levels and efficient grid synchronization, the PI controller is employed to align actual and reference power values.

2. Proposed System Methodology

Fig. 1 depicts the novel DFIG based WECS with ANN controller to optimize energy conversion and ensure efficient grid integration. The AC supply from DFIG is provided to PWM rectifier converts AC into a DC supply. The ANN controller effectively manages the wind turbine pitch through real-time blade angle changes. The DC power is delivered to three-phase VSI to convert it into AC power. Then, the PI controller is exploited for maintaining a steady DC link voltage and assures precise grid synchronization by matching the actual power values with the reference values. Furthermore, the LC filter is employed to avert harmonic distortion that enhances the output power quality.

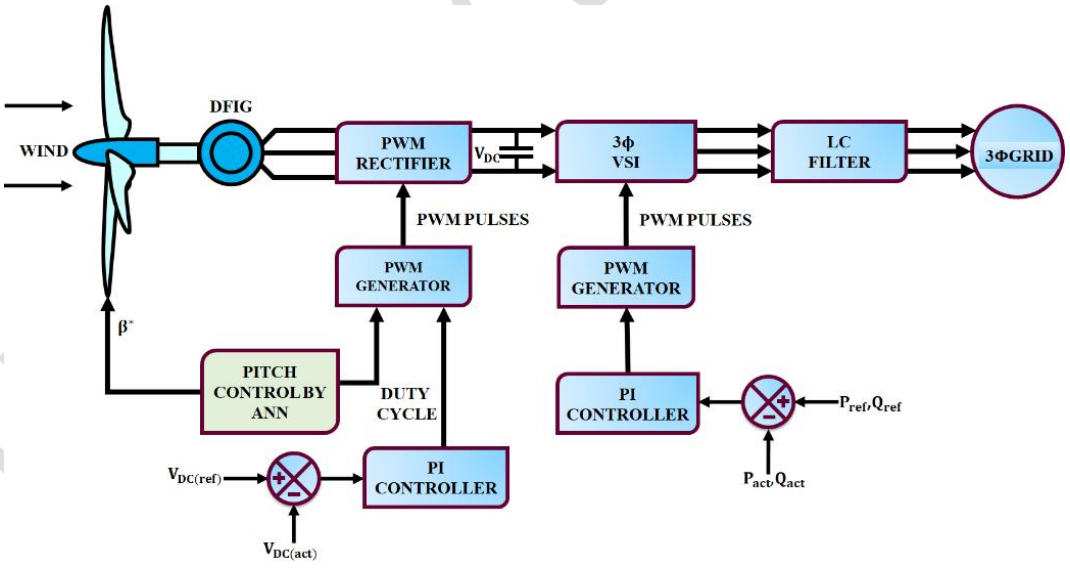

Fig. 1. DFIG Based WECS

To maximize energy capture and minimize mechanical loads, a ANN-based controller governs the turbine blade pitch angle. The PWM generator supports the rectifier and inverter by generating precise switching

pulses to assure effective operation under varying conditions. To maintain operational stability and optimize energy conversion, the control system integrates feedback loops at multiple levels. It not only improves dynamic performance but also enhances resilience against disturbances, ensuring reliable and efficient grid integration.

2-1- DFIG based WECS

DFIG is transforms the kinetic energy of moving air into mechanical energy that is delivered to DFIG, where it is transmuted into electrical power for grid integration or local use. The expression (1) is used for determining mechanical power,

$$P_m = 0.5\,pAC_p\left(\lambda,\beta\right)V_{wind}^3 \tag{1}$$

Where air density id ρ, the area swept out by turbine blade is A, wind speed is v_{wind} and power coefficient is $C_p\left(\lambda,\beta\right)$. It is dependent on two variables the blade pitch angle is β and tip speed ratio is λ.

$$\lambda = \Omega.R \big/ v_{wind} \tag{2}$$

Where, radius of blade is R and angular speed is Ω.

$$C_p\left(\lambda,\beta\right) = C_1\left(\frac{C_2}{\lambda_i} - C_3\beta - C_4\right)exp\left(\frac{-C_5}{\lambda_i}\right) + C_6\lambda \tag{3}$$

Where,

$$\frac{1}{\lambda_i} = \left(\frac{1}{\lambda + 0.08\beta} - \frac{0.035}{\beta^3 + 1}\right) \tag{4}$$

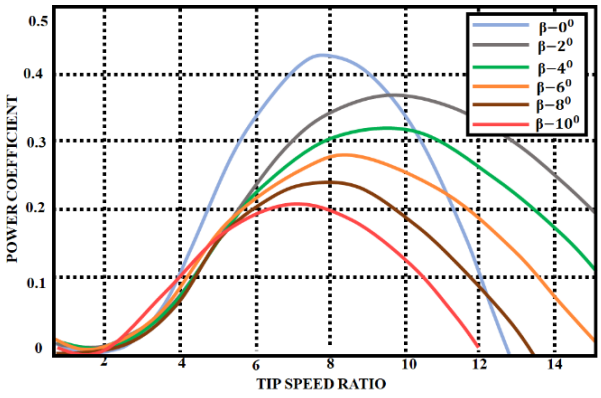

Fig. 2. Power Coefficient Curve

The power coefficient and power characteristics curve of WT are showed in Fig. 2 and Fig. 3. The nonlinear power coefficient is expressed as a function of λ and is based on the aerodynamics of turbine blades. The relationship between transmitted power, rotational speed and mechanical torque is,

$$T_m = P_m / \Omega \tag{5}$$

The optimal angular speed is expressed as,

$$\Omega_{opt} = \lambda_{opt} v_{wind} / R \tag{6}$$

The maximum mechanical power is,

$$P_{m\_max} = 0.5 p A C_{pmax} v_{wind}^3 \tag{7}$$

An asynchronous generator with a wound rotor is called a DFIG. While the rotor is connected via the converter, the stator and grid are connected directly. The DFIG dynamic model represented in an arbitrary rotating frame is simplified by using the following formula:

$$I_{ds} R_s + \frac{d}{dt}\varphi_{ds} - \varphi_{qs}\omega_s = V_{ds} \tag{8}$$

$$I_{qs} R_s + \frac{d}{dt}\varphi_{qs} + \varphi_{qs}\omega_s = V_{ds} \tag{9}$$

$$I_{ds}R_r + \frac{d}{dt}\varphi_{dr} - \varphi_{qs}\left(\omega_s - \omega_r\right) = V_{dr} \tag{10}$$

$$I_{qs}R_r + \frac{d}{dt}\varphi_{qr} - \varphi_{ds}\left(\omega_s - \omega_r\right) = V_{qr} \tag{11}$$

The synchronous reference frame is represented by d and q, whereas the stator and rotor indices are specified using s and r. Resistance is denoted by R, while electrical frequency, flux, current, and voltage are represented by the symbols ω, φ, I and V, respectively." The flux is defined as,

$$I_{ds}L_s + I_{dr}M = \varphi_{ds} \tag{12}$$

$$I_{qs}L_s + I_{qr}M = \varphi_{qs} \tag{13}$$

$$I_{dr}L_r + I_{ds}M = \varphi_{dr} \tag{14}$$

$$I_{qr}L_r + I_{qs}M = \varphi_{qr} \tag{15}$$

Where, inductance and mutual inductance is indicated by M and L.

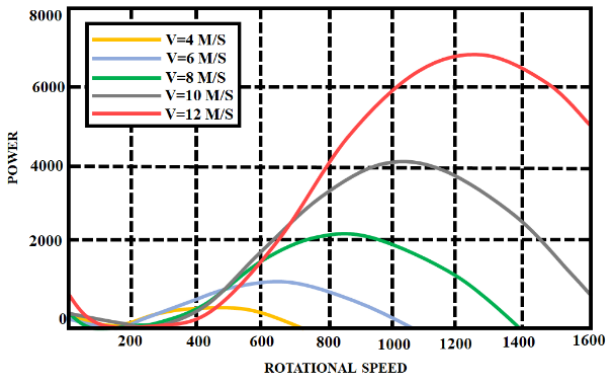

Fig. 3. Wind Turbine Power Characteristics Curve

The mechanical analysis is,

$$J\frac{d\Omega}{dt} = T_a - T_{em} - f\Omega \tag{16}$$

10.22060/EEJ.2026.24404.5701

Where, speed of generator is Ω, electromagnetic torque is T_{em} and turbine's total inertia is J . Then, T_{em} becomes,

$$T_{em} = p\frac{M}{L_s}\left(\phi_{qs} I_{dr} - \phi_{ds} I_{qr}\right) \tag{17}$$

Grid side converters and rotor-side converters are two essential parts of a DFIG system that manage the complex process of controlling energy flow between the grid, generator, and load. In order to achieve this, both converters are diligently managed by PI controllers, which are well-known for their dependability and effectiveness in control systems. The difference between the intended and actual system states is continuously evaluated by these PI controllers. They are able to modify the parameters of converters in real time by computing an error signal that represents this discrepancy. Additionally, PWM rectifier is employed for converting DFIG system's AC output into steady DC power. In order to control DC output voltage, this rectifier meticulously modifies the width of voltage pulses, guaranteeing a steady and continuous power supply.

2-2- Pitch control by ANN controller

One efficient way to control or limit turbine performance in high wind speeds is to modify the blades' pitch angle. Pitch servos, which is electrical or hydraulic systems, are used to move the blades into the required positions. Blade pitch modifications with rotational speeds of roughly 5–10º/s are anticipated during typical operation. In this case, a pitch rate of 8º/s is selected to prevent excessive loads during standard regulating processes. Pitch control, either active or passive, is utilized to safeguard the mechanical and electronic systems and capture as much energy as feasible. Pitch, speed, acceleration, and deceleration are managed to lessen the electrical current peaks and the mechanical tensions in the bucket, tower, and blades.

2-3- Passive control of pitch

The wings' angle of attack against the wind is fixed, and the blades are fastened to the hub. When wind speed surpasses a rated value, the rotor's aerodynamic design loses efficiency.

10.22060/EEJ.2026.24404.5701

2-4- Active control of pitch

When the output power is too high or too small, the blades spin to vary the angle of attack with the wind. To retain a consistent power output, the blades must be able to shift by a fraction of a degree at a time, which corresponds to a alteration in wind speed. The active pitch control system functions in a particular range of wind speeds. This research uses active pitch control for regulating the pitch of WT. The various control loops of WT is provided in Fig. 4. The four areas of operation is depicted in Fig. 5. Region I denotes wind speeds below the minimum needed to initiate rotation and at which no power is produced. When this speed is surpassed, the rotor begins to rotate and moves into region II, where the generator rotates at its normal speed and is enclosed by the starting and cutting speeds. The third area covers the nominal speed to the stoppage speed, or the maximum speed at which rotation is necessary for safety and design. Lastly, the IV region, where a mechanical brake is required for the wind turbine assembly's safety. A feedback control system's objective is to lower the error e(k) among any variable and its set to zero.

The error is calculated as,

$$e(t) = \omega_{ref} - \omega_{rotor}(t) \tag{18}$$

The first-order delay system or an integrator is a pitch actuator with a time constant τ_c, which is estimated as,

$$\frac{d\beta}{dt} = -\frac{1}{\tau_c}\beta + 1\frac{1}{\tau_c}\beta_{ref} \tag{19}$$

Where, maximum and minimum pitch angles are indicated by β_{max} and β_{min}, $\left(\frac{d\beta}{dt}\right)_{min} \le \frac{d\beta}{dt} \le \left(\frac{d\beta}{dt}\right)_{max}$ and $\beta_{min} \le \beta \le \beta_{max}$.

10.22060/EEJ.2026.24404.5701

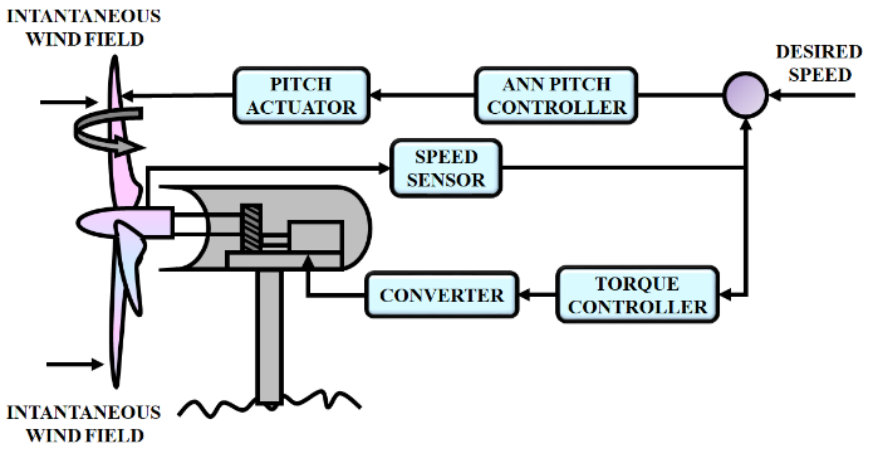

Fig. 4. WT's Standard Control Loops

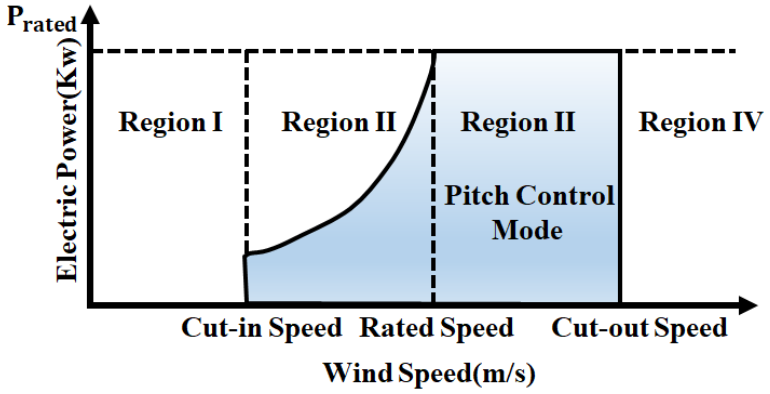

Fig. 5. Wind Turbine Operating Regions

ANN is utilized in this study to achieve nonlinear, time-varying input-output mapping, enabling effective control of the pitch angle in a wind energy system. Wind turbine generating systems exhibit highly nonlinear dynamics, as discussed earlier, making ANN an appropriate choice for pitch regulation. The control method leverages the inverse relationship between the pitch angle and other variables, such as electric power, to serve as the foundation of the developed controller.

$$\hat{\beta} = h^{-1}\left(\hat{v}, w, P_e\right) \tag{20}$$

10.22060/EEJ.2026.24404.5701

Sensors measure the generating power P_e and rotating speed w_m, while wind speed models forecast wind speed v. The set of wind speed values and set of pitch angle's historical values are used to determine the control input, which is denoted as,

$$BIC(p,q) = \chi^2 + k \cdot \ln(\mathrm{n}) \tag{21}$$

The Bayesian Information Criterion (BIC) uses p and q to signify the autoregressive orders and moving average processes, while k denotes the number of parameters in the statistical model. Predicted wind speed is exploited to determine the desired rotor speed, and historical data, including pitch angles, rotor speed, and real power output, are input into the ANN controller.

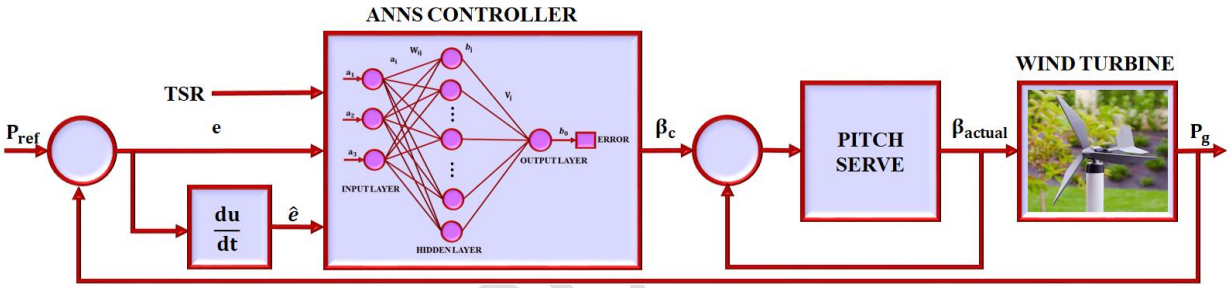

Fig. 6 Structure of ANN Base Pitch Controller

The input, hidden and output layers are the layers presented in ANN controller. The number of neurons in hidden layers are 10 to 40 and input layer has 3 inputs. The transfer function is obtained by tangent sigmoid function as,

$$\overrightarrow{f_1} = \frac{2}{\left(1+e^{-2x_j}\right)} - 1 \tag{22}$$

The output layer's transfer function is obtained by using sigmoid function as,

$$\overrightarrow{f_2} = \frac{2}{\left(1+e^{-x_0}\right)} \tag{23}$$

The output of neuron y is,

$$y = \vec{f}_2\left(v_j \vec{f}_1\left(w_{ij}\vec{a}_i + \vec{b}_j\right) + \vec{b}_o\right) \tag{24}$$

The ANN is trained offline using a dataset that covers the entire operational range of the WTDFIG system, as depicted in Fig.6. In this system, sensors identify the sample point of P_e and w_m and the wind speed ARMA model provides the v .

2-5- PI CONTROLLER

A PI controller comprises the control error based on settling value and process output and makes output according to error's proportion and integral, as revealed in Fig.7. The control signal is,

$$K_P e(t) + K_i \int_0^t e(t)dt + u_0 = u(t) \tag{25}$$

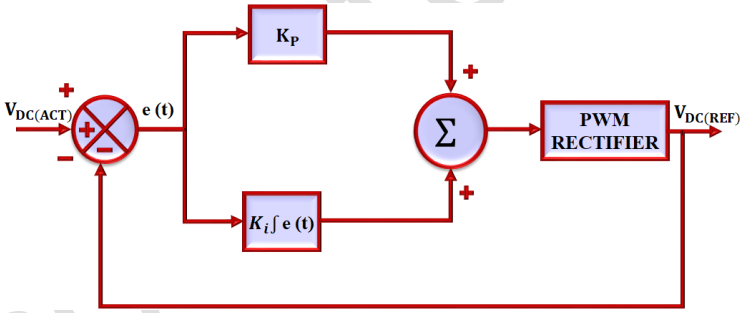

Fig. 7 Structure of PI Controller

Where, the integral parameter is K_i, initial output is u_0 and proportion parameter is K_P . The error at time t is,

$$y_{sp}(t) - y(t) = e(t) \tag{26}$$

Where, the set point is $y_{sp}(t)$ and process output is $y(t)$. The transfer function of PI controller is,

$$G_c(s) = \frac{U(s)}{E(s)} = K_P + \frac{K_i}{S} \tag{27}$$

3. Result and Discussions

The proposed system introduces DFIG-based WECS integrated with advanced control strategies to optimize energy conversion and ensure efficient grid integration. For maximum power extraction under varying wind conditions, reducing mechanical stress, an ANN-based pitch controller dynamically adjusts turbine blade angles. The MATLAB/Simulink simulations reveals the system's performance based on the parameters denoted in Table 1 and Table 2.

Table 1. WECS's Parameter Specifications

Parameters	**Values**	**Parameters**	**Values**
Nominal power	$10kW$	Line voltage	415V
Frequency	50Hz	Gear ratio	100
Turbines	4	Tip speed ratio	7
Power coefficient	0.4421	Pole pair	2

Table 2. ANN controller's Parameter Specifications

Parameters	**Values**	**Parameters**	**Values**
Activation function	ReLU	Hidden layers	3
Neurons per layer	15	Learning rate	0.005
Training algorithm	Adam optimizer	Sampling time	0.5s
Pitch actuation time	$8^{\circ}/s$	Momentum parameter	0.9
Maximum iteration	200 epochs	Error threshold	0.0001

10.22060/EEJ.2026.24404.5701

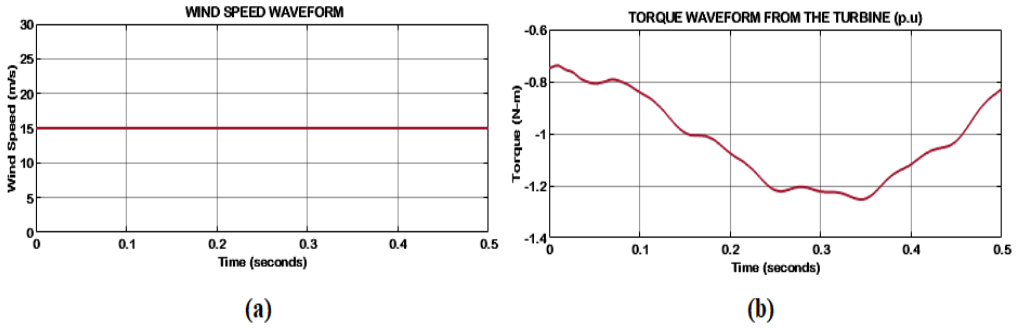

Fig. 8. Waveforms of (a) Wind speed and (b) Wind turbine torque

Fig. 8(a) reveals the wind speed is stable at 15 m/s. For a reliable analysis and control process by maintaining stable aerodynamic input to the wind turbine, this steady wind speed provides a uniform operating condition. Fig. 8(b) has fluctuations within the range of -1.3 Nm to -0.7 Nm.

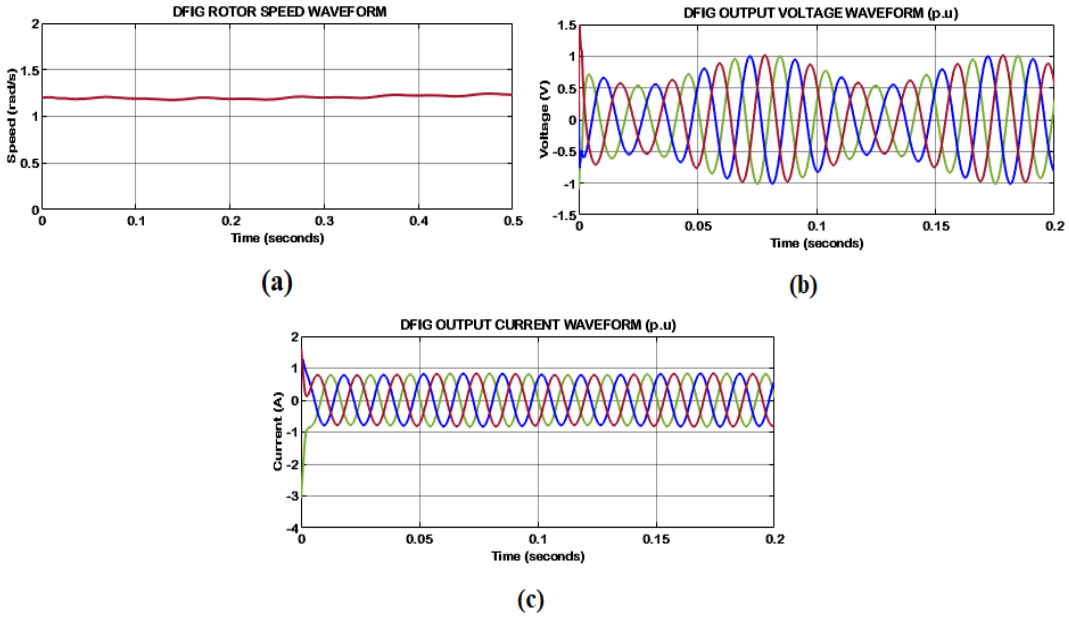

Fig. 9. Waveforms of DFIG for (a) Rotor Speed (b) Output Voltage and (c) Current

Fig. 9 offers the various operational characteristics of DFIG during energy conversion. The rotor speed is settled at 1.25 rad/s, denotes the stable operation of the rotor under given conditions. The waveform of

voltage indicates a balanced and stable voltage generation. The current waveform has stable amplitude and frequency.

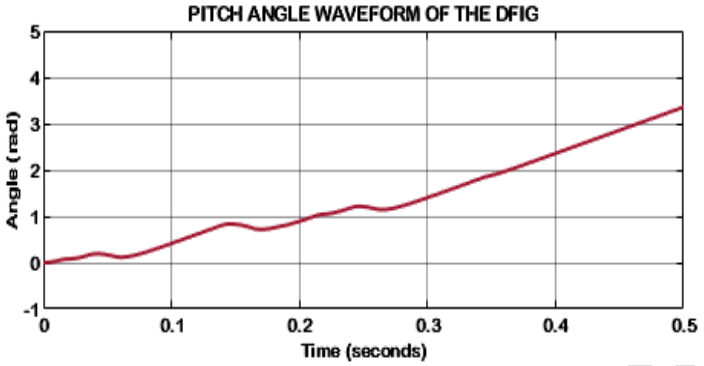

Fig. 10. Pitch Angle of DFIG

Fig. 10 represents the pitch angle of DFIG with minor fluctuations observed in the early stage. It reveals that the dynamic adjustments by the control system in response to variations in system requirements. The improvement in pitch angle denote the ANN controller optimizing the blade angles to sustain efficient energy extraction and alleviate mechanical stress on WT.

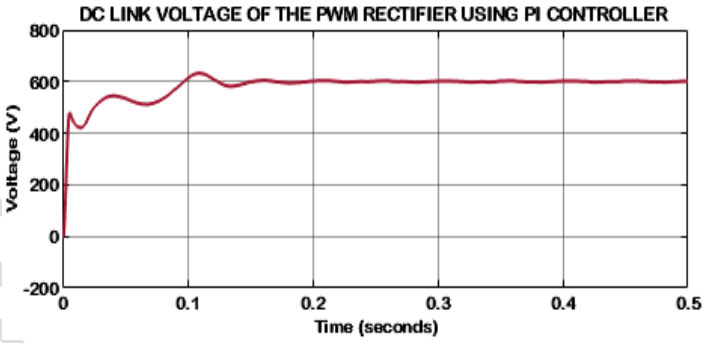

Fig. 11. DC Link Voltage Waveform

10.22060/EEJ.2026.24404.5701

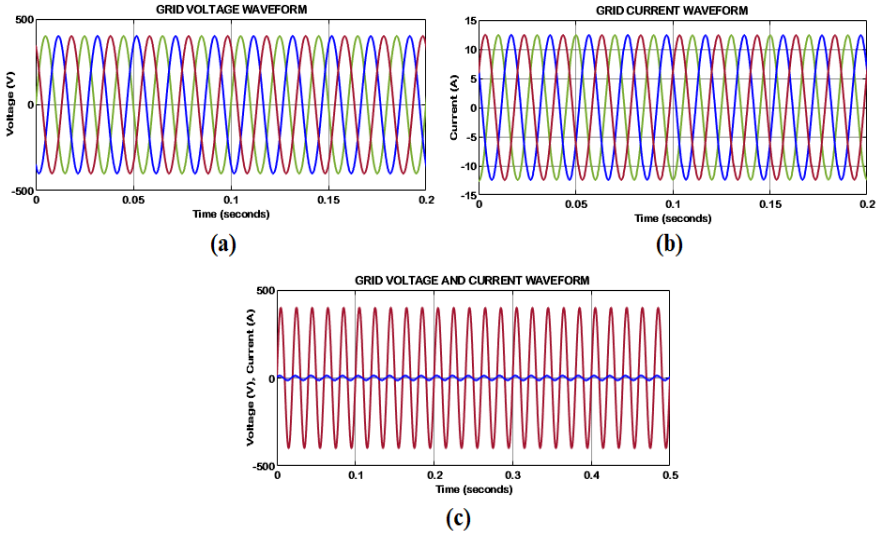

Fig. 12. Waveforms of Grid for (a) Voltage (b) Current and (c) Single Phase

The behaviour of the DC link voltage is depicted in Fig. 11, it stabilizes at 600V. It assures efficient energy conversion and compatibility with grid necessities. Fig. 12 illustrates the behaviour of grid parameters when integrated with WECS. The voltage and current are stable. An efficient power transfer with minimal reactive power is offered by alignment of voltage and current in phase.

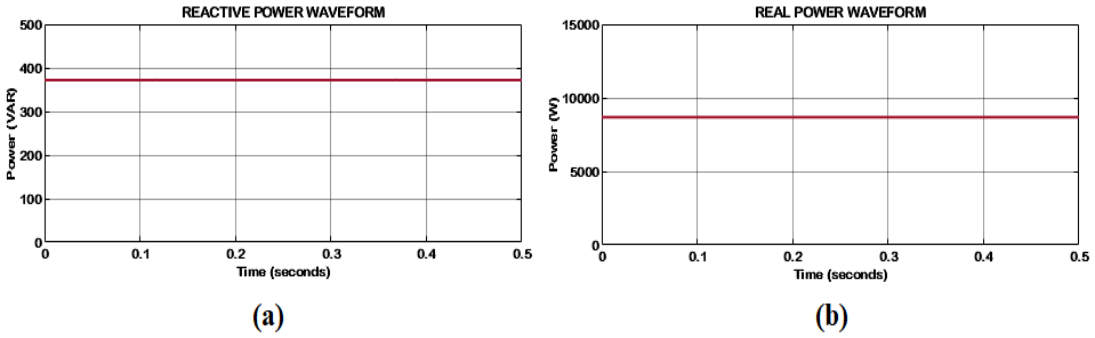

Fig. 13. Waveforms of Real and Reactive Power

The waveforms **of r**eal and reactive power is represented in Fig. 13. It denote that the system effectively manages both real and reactive power under steady conditions. It reveals the development of control approach to optimize power generation and sustain stability of grid.

10.22060/EEJ.2026.24404.5701

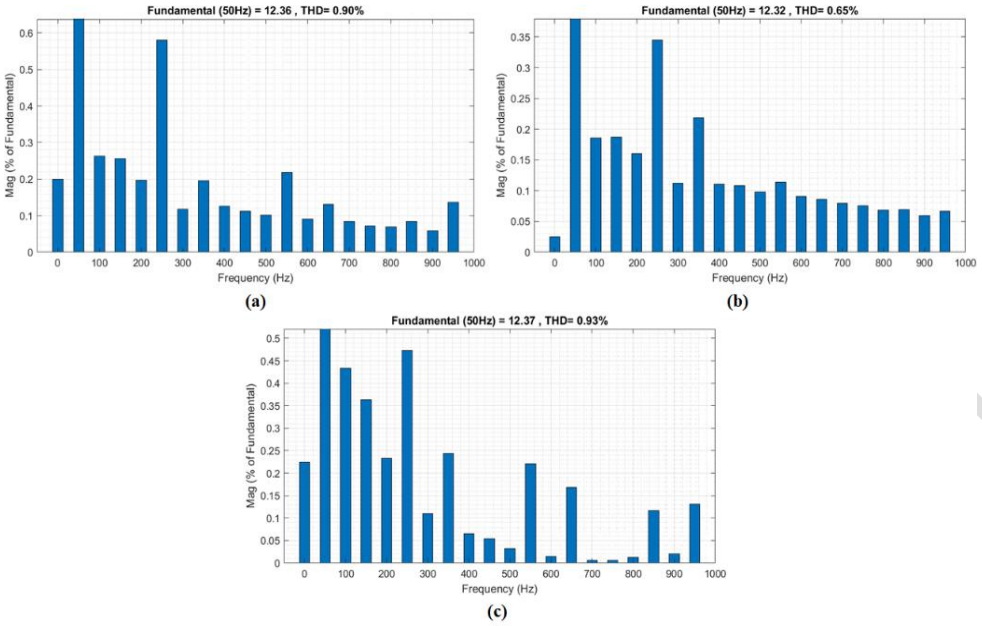

Fig. 14. THD Waveforms

The waveforms of THD **is** displayed in Fig. 14. The R, Y, and B phases maintaining values of 0.90%, 0.65%, and 0.93%, indicates the better power quality.

Table 3. Performance Evaluation of Controllers for Pitch Angle Regulation

Parameter	**PI controller**	**PID controller**	**ANN controller**
Output power stability (W)	10,000 ± 25	10,000 ± 15	10,000 ± 5
Torque fluctuations (Nm)	±0.4	±0.25	±0.1
Settling time (s)	0.35	0.25	0.15
Overshoot (%)	10%	6%	2%
Mechanical stress (kNm)	85	70	50
Pitch Actuation Rate (°/s)	12	10	8
Simulation time efficiency	85%	90%	95%

The ANN controller attains the most stable output power with minimal torque fluctuations, as denoted in Table 3. Also, it provides the quickest settling time and reduced overshoot assures a precise response to

10.22060/EEJ.2026.24404.5701

changes. The ANN controller is computationally efficient and highly adaptable with the maximum simulation time efficiency than PI and PID controllers.

3-1- Assessment of the developed work under turbulent intensity

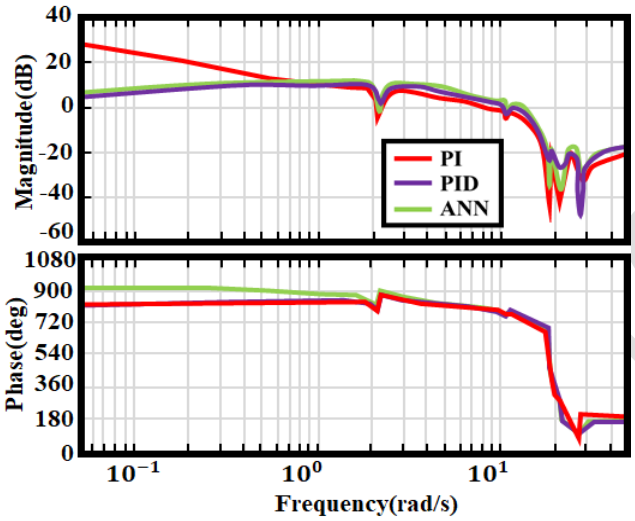

Fig. 15. Evaluation of Frequency Domain

Fig. 15 depicts an evaluation of frequency domain, denotes that the ANN controller outperform the PI controller in alleviating Blade-Root Bending Moments (BRBMs) at a wind speed of 16 m/s. The PI controller has maximum magnitude and superior phase lag, predominantly in the low-frequency range, representing reduced effectiveness in handling high and dynamic -frequency loads. Thus, the ANN controller attain small magnitudes over the frequency, proving better load suppression and adaptability.

10.22060/EEJ.2026.24404.5701

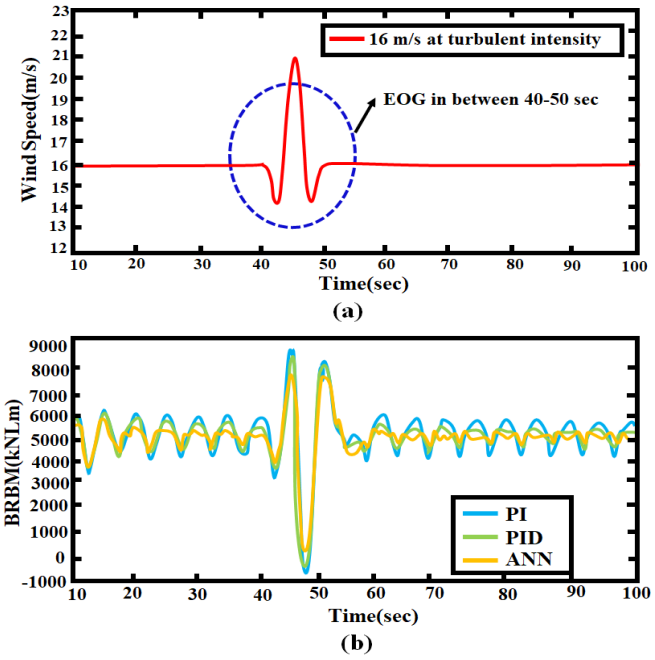

Fig. 16. Wind Speed and Blade-Root Bending Moments at 16 M/S and Turbulent Intensity

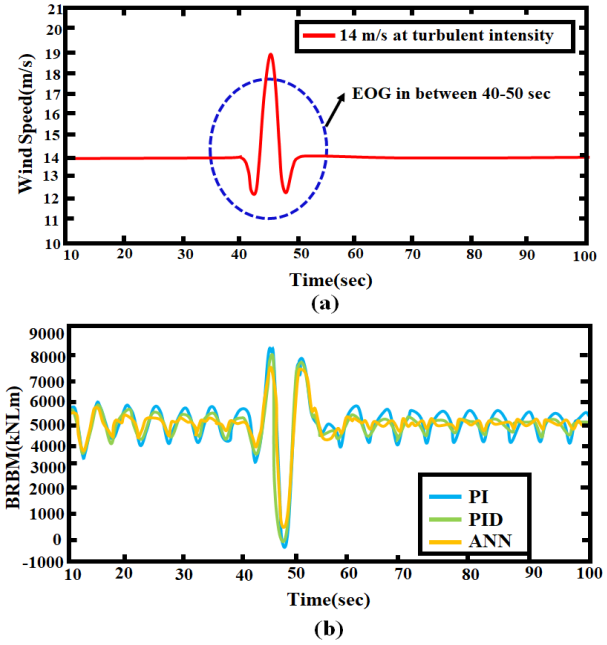

Fig. 17. Wind Speed and Blade-Root Bending Moments at 14 M/S and Turbulent Intensity

The response of wind turbines to an Extreme Operating Gust (EOG) at a wind speed of 16 m/s with turbulent intensity is depicted in Fig. 16. There is a sharp spike between 40 and 50 s, at this period, the BRBMs

10.22060/EEJ.2026.24404.5701

experience significant fluctuations. The Ann controller has better performance by reducing BRBM peaks and ensuring smoother recovery post-gust, emphasising its adaptability. The lower efficiency in mitigating extreme loads are indicated by a PI controller that has highest BRBM magnitudes. Fig. 17 reveals the response of EOG at wind speed of 14m/s with turbulent intensity. The ANN controller manage transient aerodynamic conditions, assures operational stability and structural safety.

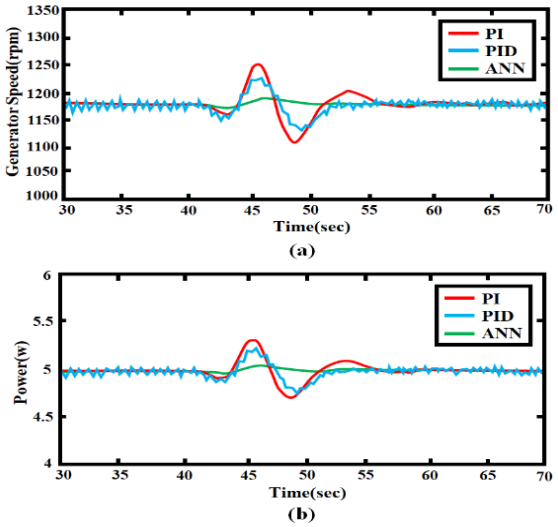

Fig. 18. Dynamic Response and Power Output to EOG at 14 M/S Wind Speed

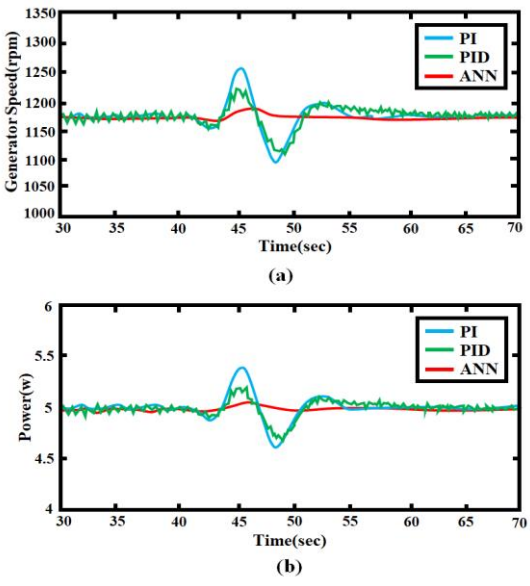

Fig. 19. Dynamic Response and Power Output to EOG at 16 M/S Wind Speed

The responses of PI, PID, and ANN controllers during EOG at 14 m/s wind speed is shown in Fig. 18. The PI controller has oscillations and sluggish recovery in power output and generator speed, representing poor performance under gust conditions. The ANN controller has superior performance, sustaining minimal deviations and consistent power regulation. Fig. 19 displays the response of generator speed and power output to EOG at a wind speed of 16 m/s. Here, the ANN controller has best performance by sustaining reduced deviations and smooth recovery.

Table 4. Efficacy Evaluation of Controllers

Parameters	**PI controller**		**PID controller**		**ANN controller**	
	14 m/s	**16 m/s**	**14 m/s**	**16 m/s**	**14 m/s**	**16 m/s**
Standard deviation	0.1815	0.1835	0.0786	0.0824	0.0205	0.0208
% reduction	-	-	56.74%	55.10%	88.70%	88.65%

The effectiveness of PI, PID and ANN controllers are depicted in Table 4. The PI controller has highest standard deviation while PID controller has reducing standard deviations to 0.0786 at 14 m/s. but, the ANN controller minimize generator speed fluctuations and sustain stability under turbulent conditions.

Table 5. Controller Performance in Managing Tilt and Yaw Moment Fluctuations under Turbulence

Standard Deviation (kNm)	**Controller**	**At Wind Speed (14 m/s)**	**At Wind Speed (16 m/s)**
Tilt moment	PI controller	1.265×10^3	1.428×10^3
	PID controller	1.238×10^3	1.372×10^3
	ANN controller	1.184×10^3	1.287×10^3
Yaw moment	PI controller	1.202×10^3	1.386×10^3
	PID controller	1.171×10^3	1.370×10^3
	ANN controller	1.123×10^3	1.255×10^3

The performance of PI, PID and ANN controller is displayed in Table 5. The ANN controller steadily outperforms the others attaining the lowest standard deviations of 1.184×10^3 kNm at 14 m/s and 1.287×10^3 kNm at 16 m/s, representing superior stability and load reduction for tilt moment. The ANN controller attains the better performance with deviations to 1.123×10^3 kNm at 14 m/s and 1.255×10^3 kNm at 16 m/s in yaw moments. It demonstrates that the ANN controller's superior ability to manage dynamic loads and sustain system stability under turbulence.

Table 6. Performance Analysis of Controllers

Approaches	**MSE**	**RMSE**
PID	1.296E-7	0.00036
RNN	3.28E-11	5.54E-06
Proposed	0.00013	0.0254

The performance analysis of controllers with Mean Squared Error (MSE) and Root Mean Squared Error (RMSE) are revealed in Table 6. The proposed approach has the lowest MSE and RMSE of 0.00013 and 0.0254, indicating the overall performance of the system is enhanced.

Table 7. Analysis of THD

Approaches	**THD**
FOSMC	1.38%
SOSMC	1.28%
TOSMC	1.06%
Proposed	0.65%

Table 7 displays the analysis of THD for FOSMC, SOSMC, TOSMC and proposed approach, which has the lowermost THD of 0.65% among others, denoting the power quality is enhanced maximizing power generation.

4. Conclusion

A novel pitch control technique based on ANN for enhancing the efficiency of wind energy systems is developed in this research. By dynamically regulating the blade pitch to optimal angles, the ANN aids in enhancing the efficacy of energy conversion from wind to electrical power, safeguarding reliable and stable operation. The AC voltage from wind turbines is transformed into DC voltage by PWM rectifier, regulate the magnitude of output voltage. The DC power produced by the PWM rectifier is given to an inverter that transforms it into an AC power, guarantees that the power from the wind turbine is well-suited with the electrical grid. Moreover, the output achieved is transformed into AC using 3ϕ VSI and by achieving grid synchronization with the help of PI controller, DC link voltage is delivered to a grid. The results have applied in MATLAB/ Simulink, proves that the developed work provides the better performance. Simulation results validate the superior performance of the ANN controller over conventional PI and PID controllers, demonstrating reduced generator speed fluctuations, lower mechanical stress, and enhanced power stability. The ANN controller has minimal overshoot, quicker response times and better dynamic stability under extreme wind events. Nevertheless, tuning of ANN controller is more complex and intensive, needs more sophisticated hardware for real world applications.

References

[1] S. Al-Janabi, A. F. Alkaim, and Z. Adel, “An Innovative synthesis of deep learning techniques (DCapsNet & DCOM) for generation electrical renewable energy from wind energy”, 2020 soft Computing, vol. 24, no. 14, pp. 10943-10962.

[2] W. S. Udo, J. M. Kwakye, D. E. Ekechukwu, and O. B. Ogundipe, “Optimizing wind energy systems using machine learning for predictive maintenance and efficiency enhancement”, 2024 Journal of Renewable Energy Technology, vol. 28, no. 3, pp. 312-330.

[3] R. Gianto, “Steady-state model of DFIG-based wind power plant for load flow analysis”, 2021 IET Renewable Power Generation, vol. 15, no. 8, pp. 1724-1735.

[4] N. A. Dwijendra, T. J. Abduladheem, A. M. B. S. Abed, Bashar, A. J. Al-Nussairi, A. T. Hammid, A. Shamel, and K. F. Uktamov, “Improving the transition capability of the low-voltage wind turbine in the sub-synchronous state using a fuzzy controller”, 2022 Clean Energy, vol. 6, no. 4, pp. 682-692.

[5] S. Sarkar, B. Fitzgerald, and B. Basu, “Individual blade pitch control of floating offshore wind turbines for load mitigation and power regulation”, 2020 IEEE Transactions on Control Systems Technology, vol. 29, no. 1, pp. 305-315.

[6] H. Ren, B. Hou, G. Zhou, L. Shen, C. Wei, and Q. Li, “Variable pitch active disturbance rejection control of wind turbines based on BP neural network PID”, 2020 IEEE Access, vol. 8, pp. 71782-71797.

[7] M. Elsisi, M. Q. Tran, K. Mahmoud, M. Lehtonen, and M. F. Darwish, “Robust design of ANFIS-based blade pitch controller for wind energy conversion systems against wind speed fluctuations”, 2021 IEEE Access, vol. 9, pp. 37894-37904.

[8] H. Badihi, Y. Zhang, P. Pillay, and S. Rakheja, “Fault-tolerant individual pitch control for load mitigation in wind turbines with actuator faults”, 2020 IEEE Transactions on Industrial Electronics, vol. 68, no. 1, pp. 532-543.

[9] D. Bustan, and H. Moodi, “Adaptive interval type-2 fuzzy controller for variable-speed wind turbine”, 2020 Journal of Modern Power Systems and Clean Energy, vol. 10, no. 2, pp. 524-530.

[10] C. Zhang, and F. Plestan, “Individual/collective blade pitch control of floating wind turbine based on adaptive second order sliding mode”, 2021 Ocean Engineering, vol. 228, pp. 108897.

[11] J. E. Sierra-García, and S. Matilde, “Improving wind turbine pitch control by effective wind neuro-estimators”, 2021 IEEE Access, vol. 9, pp. 10413-10425.

[12] V. L. Narayanan, and R. Ramakrishnan, “Design and implementation of an intelligent digital pitch controller for digital hydraulic pitch system hardware-in-the-loop simulator of wind turbine”, 2021 International Journal of Green Energy, vol. 18, no. 1, pp. 17-36.

[13] Z., Lin, and X. Liu, “Wind power forecasting of an offshore wind turbine based on high-frequency SCADA data and deep learning neural network”, 2020 Energy, vol. 201, pp. 117693.

[14] P. Korkos, M. Linjama, J. Kleemola, and A. Lehtovaara, “Data annotation and feature extraction in fault detection in a wind turbine hydraulic pitch system”, 2022 Renewable Energy, vol. 185, pp. 692-703.

[15] P. Chen, D. Han, F. Tan, and J. Wang, “Reinforcement-based robust variable pitch control of wind turbines”, 2020 IEEE Access, vol. 8, pp. 20493-20502.

[16] M. Lara, J. Garrido, M. L. Ruz, and F. Vázquez, “Adaptive pitch controller of a large-scale wind turbine using multi-objective optimization”, 2021 Applied Sciences, vol. 11, no. 6, pp. 2844.

[17] A. Fekih, S. Mobayen, and C. C. Chen, “Adaptive robust fault-tolerant control design for wind turbines subject to pitch actuator faults”, 2021 Energies, vol. 14, no. 6, pp. 1791.

[18] C. Zhang, and F. Plestan, “Adaptive sliding mode control of floating offshore wind turbine equipped by permanent magnet synchronous generator”, 2021 Wind Energy, vol. 24, no. 7, pp. 754-769.

[19] Q. Hawari, T. Kim, C. Ward, and J. Fleming, “A robust gain scheduling method for a PI collective pitch controller of multi-MW onshore wind turbines”, 2022 Renewable Energy, vol. 192, pp. 443-455.

[20] J. E. Sierra-Garcia, M. Santos, and R. Pandit, “Wind turbine pitch reinforcement learning control improved by PID regulator and learning observer”, 2022 Engineering Applications of Artificial Intelligence, vol. 111, pp. 104769.

[21] N. M. Mousa, Y. I. El-Shaer, and M. A. El-Sebah, “A proposed controller for pitch angle of wind turbine,” 2023 WSEAS Transactions on Systems and Control, vol. 18, pp. 527-539.

[22] A. Khurshid, M. A. Mughal, A. Othman, T. Al-Hadhrami, H. Kumar, I. K. Arshad, and J. Ahmad, “Optimal pitch angle controller for DFIG-based wind turbine system using computational optimization techniques,” 2022 Electronics, vol.11, no. 8, pp. 1290.

[23] C. Roh, “Deep-learning-based pitch controller for floating offshore wind turbine systems with compensation for delay of hydraulic actuators,” 2022 Energies, vol.15, no. 9, pp. 3136.